Change in permeant size selectivity by phosphorylation of connexin 43 gap-junctional hemichannels by PKC

Xiaoyong Bao*, Sung Chang Lee†, Luis Reuss*, and Guillermo A. Altenberg†‡§

*Department of Neuroscience and Cell Biology, †Division of Nephrology and Hypertension, Department of Internal Medicine, and ‡Sealy Center for Structural Biology and Molecular Biophysics, University of Texas Medical Branch, Galveston, TX 77555-0437

Edited by Michael V. L. Bennett, Albert Einstein College of Medicine, Bronx, NY, and approved January 8, 2007 (received for review April 18, 2006)

Gap-junctional channels, permeable to large hydrophilic solutes of up to $M_r \approx 1{,}000$, are responsible for cell-to-cell communication. Phosphorylation of connexin 43 (Cx43) by PKC abolishes the permeability of gap-junctional channels and hemichannels to large hydrophilic solutes, but not to small inorganic ions. Here, we report on a methodology to produce purified hemichannels of controlled subunit composition and apply it to the generation of hemichannels with variable number of PKC-phosphorylated subunits. The subunit composition was determined by luminescence resonance energy transfer. We show that all Cx43 subunits in the hemichannel hexamer have to be phosphorylated to abolish sucrose (M_r 342) permeability. We also show that the hemichannel pores with all subunits phosphorylated by PKC have a sizable diameter, allowing for permeation of the small hydrophilic solute ethyleneglycol (M_r 62). These results indicate that phosphorylation of Cx43 by PKC alters the hemichannel size selectivity and explain why PKC activity affects dye transfer between cells without consistent effects on electrical communication.

luminescence energy transfer | membrane protein | transport

Gap-junctional channels are responsible for cell-to-cell communication (1). They are formed by head-to-head docking of two connexin hexamers (hemichannels or connexons), one from each of the neighboring cells (1–3). Gap-junctional channels are permeable to large hydrophilic solutes of up to $M_r \approx$ 1,000, depending on their isoform composition (1, 4). Connexin 43 (Cx43) is expressed in cells from organs such as brain, myocardium, and kidney, and in vascular endothelial cells, where it mediates cell-to-cell communication, a process essential for development and organ function (5–7). Uncoupled hemichannels have been shown to exist in several cell types (see below). Activation of these large nonselective Cx43 hemichannels, e.g., during ischemia, may overwhelm the normal membrane-transport mechanisms and alter intracellular composition, contributing to cell injury. This notion is supported by data on cardiomyocytes (8, 9), astrocytes (10), and renal proximal tubule cells (11) that show Cx43 hemichannel activation by ATP depletion. One possibility is that ATP depletion activates the Cx43 hemichannels by decreasing their phosphorylation state (12), although other possibilities have been proposed (13).

Activation of PKC decreases cell-to-cell movement of hydrophilic permeability probes, such as fluorescent dyes (dye coupling), while electrical communication between cells persists (reviewed in ref. 14). These direct effects are independent of the effects of phosphorylation on trafficking, assembly, and/or degradation (15). Single-channel studies have shown that stimulation of PKC decreases the frequency of the dominant (≈100 pS) conductance state, favoring a lower conductance state (≈50 pS) of Cx43 gap-junctional channels (reviewed in ref. 14). This change is likely to occur concomitantly with an increase in open probability (16), which explains the lack of consistent effects of changes in PKC activity on cell-to-cell electrical communication (14, 16–18). We hypothesize that the dissociation of the effects on "large" and "small" solute permeability is the consequence of a partial reduction of the effective cross-sectional area of Cx43 hemichannels by PKC-mediated phosphorylation. To test this hypothesis, we studied the transport of hydrophilic solutes of different sizes through hemichannels formed by Cx43 either fully dephosphorylated (Cx43-dP) or fully PKC-phosphorylated (Cx43-P).

Results and Discussion

Phosphorylation of All Six Cx43 Subunits by PKC Produces a Partial Reduction of the Effective Cross-Sectional Area of the Hemichannel Pore. For the transport studies we measured retention of permeability probes after gel filtration of proteoliposomes preloaded with radiolabeled probes (19). The methodology (probe-retention studies) and experimental system (reconstituted purified hemichannels) have been described (18, 19), and additional validation is presented in supporting information (SI) *Text* and SI Fig. 6. We used sucrose as the main permeability probe because its molecular mass is in the lower side of the range of the masses of second messengers of functional significance that permeate gap-junctional channels and hemichannels. Phosphorylation by PKC of all six Cx43 subunits at Ser-368 abolishes sucrose permeability of reconstituted hemichannels (18). The absence of sucrose transport through Cx43-P hemichannels was confirmed by sucrose retention measurements. In Fig. 1, we show that the maltose permeability is abolished by PKC-mediated phosphorylation, as expected, because both disaccharides have the same molecular weight (M_r 342). The smaller probe ethyleneglycol (M_r 62), however, was permeant through hemichannels formed by either Cx43-dP or Cx43-P, indicating that a hemichannel pore of significant size remains when all six Cx43 molecules are phosphorylated by PKC. In other words, phosphorylation of all of the subunits by PKC produces a partial decrease of the cross-sectional area of the Cx43 hemichannel pore, i.e., the hemichannels remain permeable to ethyleneglycol.

Although an accurate estimation of the minimum hydrophilic pore size of Cx43-P hemichannels is complicated by the potential interaction of the permeability probes with pore-lining side chains (20), the hydrodynamic diameter of ethyleneglycol is 4.4

Author contributions: X.B. and S.C.L. contributed equally to this work; L.R. and G.A.A. designed research; X.B., S.C.L., and G.A.A. performed research; X.B., S.C.L., L.R., and G.A.A. analyzed data; and L.R. and G.A.A. wrote the paper.

The authors declare no conflict of interest.

This article is a PNAS direct submission.

Freely available online through the PNAS open access option.

Abbreviations: Cx43, connexin 43; Cx43-dP, dephosphorylated Cx43; Cx43-P, PKC-phosphorylated Cx43; decylmaltoside, *n*-decyl-β-D-maltopyranoside; DTPA, diethylenetriaminepentaacetate; EMCH, ε-maleimidocaproic acid hydrazide; LRET, luminescence resonance energy transfer.

§To whom correspondence should be addressed. E-mail: galtenbe@utmb.edu.

This article contains supporting information online at www.pnas.org/cgi/content/full/0603154104/DC1.

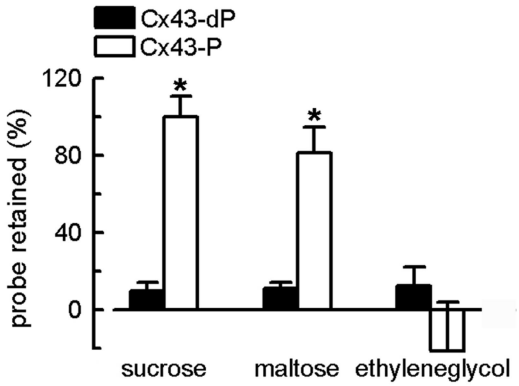

Fig. 1. Effects of PKC-mediated phosphorylation of hemichannels on their permeability to hydrophilic solutes. The proteoliposomes were loaded with radiolabeled probes, and the percent retention of the permeability probes was measured after gel filtration. Studies were performed in proteoliposomes containing hemichannels formed by fully dephosphorylated Cx43 (Cx43-dP) or Cx43 fully phosphorylated by PKC (all six Ser-368 residues phosphorylated, Cx43-P). Values were normalized to the amount of probe retained by liposomes formed by Cx43-P (statistically indistinguishable from the value measured in liposomes without hemichannels, 112 ± 9%, $n = 7$), after subtraction of the background measured in DMSO-permeabilized liposomes. Ethyleneglycol values were normalized to those in liposomes without hemichannels. The average number of hemichannels per liposome was 2.3. Data are means ± SEM of four to seven experiments. *, $P < 0.05$ compared with proteoliposomes containing Cx43-dP hemichannels.

Å (21), i.e., significantly larger than that of hydrated K^+ and Cl^- (≈3.3 Å) (22), the main ions carrying currents through gap-junctional channels. Therefore, our results explain why activation of PKC reduces dye transfer (17, 18), but has no substantial effect on cell-to-cell gap-junctional currents (14). The differential modulation of Cx43 permeability by PKC-mediated phosphorylation could reduce fluxes of organic hydrophilic solutes such as ATP, cAMP, IP3, and NAD^+ (300–700 Da molecular mass) without major effects on small-ion fluxes and electric coupling.

As mentioned in the Introduction, stimulation of PKC decreases the frequency of the dominant (≈100 pS) conductance state of Cx43 gap-junctional channels, favoring a lower conductance state (≈50 pS) (reviewed in ref. 14). It seems possible that these lower conductance channels are formed by the fully phosphorylated hemichannels permeable to ethyleneglycol that are described here. However, the level of Cx43 phosphorylation in the cells is uncertain, and it is important to point out that there is no simple correlation between the single-hemichannel conductance and the permeability to large hydrophilic solutes of hemichannels formed by different connexin isoforms (1, 23).

Evidence for Exchange of Subunits Between Solubilized Hemichannels. Given the observation that hemichannels formed by Cx43-dP are sucrose-permeable, whereas those formed by Cx43-P are not, we investigated how many Cx43 subunits in a hemichannel must be phosphorylated to abolish sucrose permeability. To this end, we generated hemichannels with a known number of PKC-phosphorylated subunits (by mixing purified Cx43-dP and Cx43-P in different proportions) and measured their sucrose permeability. Because the generation of hemichannels of controlled composition was attempted *in vitro*, it was critical to demonstrate that there is exchange between solubilized Cx43 subunits and that the composition of the reconstituted hemichannels is that expected from the ratio of Cx43-dP and Cx43-P in the mixture. Previous studies (24–27) have shown solubilization of gap-junctional plaques into hemichannels, but compared with our studies there were differences in the solubilization conditions and/or isoforms studied. One possibility to explain the apparent discrepancies is the observation that the outcome of the solubilization depends on the nature of the membranes (28). When Cx32 synthesized *in vitro* in the presence of microsomes was solubilized with dodecylmaltoside, it appeared mostly as monomers, whereas supplementation with Golgi membranes increased the amount of solubilized hexamers significantly (28). This effect was not observed for Cx26 (28), indicating that it is isoform-dependent. Insect cells have membranes of unusual properties and composition (29), which may explain why solubilization of Cx43 with several detergents yields monomers (at low concentrations), which can assemble as hexamers (at higher concentrations) that display subunit exchange. In the present study, we specifically looked at the possibility of exchange of subunits in solubilized hemichannels. Definitive evidence that exchange occurs is presented below [gel-filtration experiments, luminescence resonance energy transfer (LRET) experiments, sucrose-transport studies]. It is important to mention that this subunit exchange occurs when the subunits are solubilized, and that we do not have evidence for exchange once the purified hemichannels are reconstituted.

One potential concern is that the purified hemichannels generated from solubilized subunits differ significantly from native hemichannels in cell membranes. This concern cannot be ruled out, but we have evidence for significant functional and structural similarities between the native and purified hemichannels: (*i*) The permeability properties of native and purified Cx43 hemichannels are internally consistent, and phosphorylation of Ser-368 by PKC abolishes large-solute permeability in both purified and native hemichannels (17, 18). (*ii*) The residue at position 161 of transmembrane helix 3 is a pore-lining residue in native and purified hemichannels (*SI Text*). (*iii*) The face of transmembrane helix 3 that lines the pore is the same in native and purified hemichannels, as determined by the substituted Cys accessibility method (unpublished observations). (*iv*) The distances between homologous residues of transmembrane helix 3 in diametrically opposed subunits are entirely consistent with the structure of Cx43 gap-junctional channels [unpublished measurements using LRET, based on the same principles recently described for a study of K^+ channels (30)].

In our previous studies (18) and data shown here (Fig. 2), we have observed that at a concentration of ≈20 μM, solubilized Cx43 fused to an EGFP at the C-terminal end (Cx43-EGFP) forms hexamers, as assessed by gel filtration. The first indication of a dynamic oligomerization process was suggested by additional gel filtration studies that showed that upon rerunning the Cx43-EGFP hexamers after sample dilution, Cx43-EGFP elutes as monomers (data not shown). To demonstrate subunit exchange, we studied *n*-decyl-β-D-maltopyranoside (decylmaltoside)-solubilized hemichannels by using gel filtration chromatography. Because the difference in molecular size between Cx43-dP and Cx43-P is very small for detection by gel filtration, we mixed Cx43 with Cx43-EGFP. The ≈26-kDa EGFP increases the molecular mass significantly, allowing for detection of mixed oligomers. We have previously shown that the regulation of Cx43 by PKC-mediated phosphorylation is not affected by EGFP fusion (18). Fig. 2 shows that mixing of hemichannels formed by Cx43 with those formed by Cx43-EGFP yields hemichannels containing both Cx43 and Cx43-EGFP. The quantitative molecular mass analysis of the major peaks is consistent with Cx43 hexamers (Fig. 2, black traces), Cx43-EGFP hexamers (Fig. 2, green traces), and "mixed" Cx43/Cx43-EGFP hexamers (Fig. 2, red traces). The detergent bound to the hexamers (assessed from the difference between the calculated molecular mass and that expected from six connexins) seems to be ≈5–10% of the hexamer weight. Clearly, the Cx43:Cx43-EGFP mix localizes mostly to a peak that elutes between the hexamers of Cx43 and Cx43-EGFP. The peak of the hexamer mix is only slightly wider than those of the Cx43 and Cx43-EGFP hexamers and does not

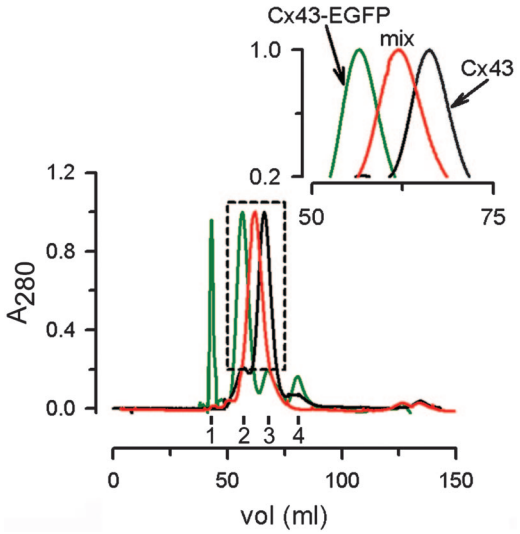

Fig. 2. Gel-filtration chromatography of hemichannel mixtures. Purified Cx43 and Cx43-EGFP gently mixed overnight at a 4:2 molar ratio, at 4°C, were analyzed by gel filtration in 0.3% decylmaltoside, 150 mM NaCl, 0.1 mM EDTA, and 10 mM Hepes/NaOH, pH 7.5. Ferritin (440 kDa, labeled 2) and aldolase (158 kDa, labeled 4) or thyroglobulin (669 kDa, labeled 1), catalase (232 kDa, labeled 3), and aldolase (158 kDa, labeled 4) were mixed with Cx43 and Cx43-EGFP, respectively, before injection into the FPLC system. Absorbance was measured at 280 nm (A_{280}) and normalized to the hexamer peak values.

extend from the Cx43-EGFP to the Cx43 peaks, indicating that it corresponds to mixed Cx43:Cx43-EGFP hemichannels and not to separate Cx43 and Cx43-EGFP that coexist without connexin exchange. Additional evidence for subunit exchange was obtained by LRET and sucrose-transport studies and is described later.

The gel-filtration experiments indicate that there is a dynamic equilibrium between subunits in solubilized hemichannels. In three independent experiments, the peak of the Cx43-EGFP:Cx43 mix ran between the Cx43 and the Cx43-EGFP hexamers peaks, but its relative location differed slightly from experiment to experiment, preventing the accurate determination of the hemichannel composition (e.g., discrimination between hemichannels containing three from those containing five Cx43-EGFP subunits was not possible).

Analysis of Hemichannel Subunit Composition by LRET. To improve the analysis of mixed hemichannels, we developed a method based on LRET, using the rare element Tb^{3+}, characterized by a long lifetime emission, as donor (31) and fluorescein as acceptor. We measured LRET between Cx43 subunits labeled with either Tb^{3+} or fluorescein to determine the composition of hemichannels based on the number of acceptor-labeled monomers per hemichannel. LRET is sensitive and independent of the connexin molecular weight and has been used in a few studies of membrane proteins to assess intersubunit and intramolecular distances (32–35). LRET has many advantages for our experiments when compared with traditional FRET (31, 32). As shown later and in *SI Text*, these advantages translate in very low background, high signal-to-noise ratio, and independence of the labeling stoichiometry (32).

For our experiments, we mixed fluorescein-labeled, Tb^{3+}-labeled and unlabeled Cx43 in different proportions. The Cx43 mixtures had a low proportion of Tb^{3+}-labeled Cx43 (0.5 mol per hemichannel), so most hemichannels had zero or one Tb^{3+}-labeled Cx43 subunit, and only a small percentage (≈8%; calculated from the binomial distribution) had more than one donor-label subunit. Under these conditions, and considering that essentially all subunits are assembled as functional hemichannels (see *Materials and Methods* and ref. 18), the amplitude of fluorescein emission caused by energy transfer from Tb^{3+} (sensitized fluorescein emission with long lifetime) depends on the number of acceptors (fluorescein-labeled Cx43 per hemichannel) and can be used to determine the subunit composition of the hemichannels. This is because all LRET under the conditions of our experiments occurs between subunits in a hemichannel. There is no intramolecular LRET because subunits are labeled with donor or acceptor separately, before mixing. Because of the long distances involved (>1,000 Å) and the high dependence of energy transfer on the distance (inversely proportional to the sixth power of the distance), significant LRET between hemichannels in solution or hemichannels in different liposomes is not expected. The absence of interhemichannel LRET was demonstrated by measuring the time course of the increase in sensitized emission upon mixing two populations of detergent-solubilized hemichannels, one labeled with Tb^{3+} and the other one labeled with fluorescein. From such experiments, a halftime of subunit exchange of ≈14 min was measured, with essentially no signal immediately after mixing. Also, there was no significant LRET when two sets of proteoliposomes, one containing donor-labeled hemichannels and another one containing acceptor-labeled hemichannels, were mixed (data not shown).

WT Cx43 contains nine Cys of which at least four are likely to form intramolecular disulfide bonds. Under the labeling conditions of most of our experiments (see *Materials and Methods*), the stoichiometry of labeling was 3.2 ± 0.1 fluorescein molecules (n = 4) or 3.1 ± 0.1 Tb^{3+} (n = 3) per Cx43. These findings suggest that only 1/3 of the Cys in WT Cx43 are accessible to the labeling reagents. In a given hemichannel containing a donor-labeled subunit, there will be energy transfer between each of the donors in the subunit and each of the acceptors in an acceptor-labeled subunit. Therefore, there will be nine energy-transfer processes between the donor subunit and each acceptor-labeled subunit. We use total energy-transfer data, without deconvoluting the individual transfers (which depend on the distances between each donor-acceptor pair). Thus, each labeled subunit in a hemichannel can be treated as a donor or acceptor, with the sensitized emission between a donor-labeled and an acceptor-labeled subunit as the sum of the energy transfer arising from the nine donor–acceptor pairs.

In experiments with WT Cx43 hemichannels in which the labeling stoichiometry was reduced to ≈1, by reducing the labeling time, a decrease in the magnitude of the signal was observed, but the relationship between LRET and the number of fluorescein-labeled subunits was not affected (data not shown). Additional data showing independence of the methodology on the labeling stoichiometry and the absence of significant background (measured on Cys-less Cx43 hemichannels) are presented in SI Fig. 6. Connexin labeling and the LRET data were also independent of whether Cx43 was dephosphorylated or PKC-phosphorylated (data not shown). Therefore, the assembly of detergent-solubilized Cx43 into hemichannels does not depend on phosphorylation, confirming our previous observations (18).

Because the energy transfer depends on the sixth power of the distance between donor and acceptor, the largest fraction of the total sensitized emission is the result of energy transfer between the Tb^{3+}-labeled subunit and the closest fluorescein-labeled subunits. However, considering a Förster distance R_0 for the Tb^{3+}–fluorescein pair of ≈45 Å, and distances between subunits in a hemichannel <100 Å, even the acceptor-labeled subunit diametrically opposed to the donor-labeled subunit contributes significantly to the total energy transfer in a hemichannel. In summary, all acceptor-labeled subunits contribute to the sensitized emission, and therefore the signal is proportional to the number of labeled subunits in the hemichannel.

Fig. 3*A* shows that, as expected, the steady-state fluorescence

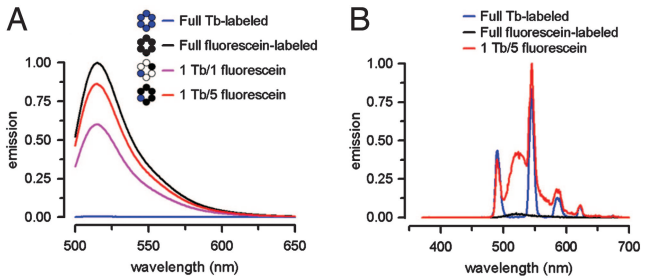

Fig. 3. LRET between Tb^{3+}- and fluorescein-labeled Cx43 subunits in hemichannels. Purified WT Cx43 solubilized in 0.3% decylmaltoside was labeled with either fluorescein maleimide or Tb^{3+}-DTPA-cs124-EMCH, by incubation for 2 h at 4°C with a 10-fold molar excess of the thiol reagents. Unreacted labels were removed by gel filtration, and unlabeled and labeled proteins were mixed in varying proportions and incubated for at least 2 h before analysis. (*A*) Steady-state fluorescence emission spectra (excitation at 490 nm). Data are normalized to the peak value of fully fluorescein-labeled preparation. (*B*) Gated emission spectra (60-μs delay after a 337-nm, 1-ns pulse from a nitrogen laser). Control experiments showed that at the concentrations present during Cx43 labeling there is no significant LRET between free Tb^{3+} and free fluorescein after gel filtration. Data were normalized to the peak value of 1 Tb/5 fluorescein-labeled preparation. Traces are representative from four independent experiments.

increases with the content of fluorescein-labeled Cx43 per hemichannel. The important result is that when the emission is measured in a gated mode (without recording during the first 60 μs after a 1-ns nitrogen laser pulse), the fluorescein emission caused by direct excitation is very low (Fig. 3*B*, black trace). This finding is expected from the short duration of the excitation pulse (1 ns) and the short lifetime of the fluorescein excited state (4–5 ns). In addition, the lack of signal from scattering of the excitation pulse and the sample autofluorescence, caused by the short excitation pulse and nanosecond lifetimes of native fluorophores, combine to contribute to a low emission background. Fig. 3*B* (blue trace) shows that lanthanide emission is in sharp peaks with interposed dark regions (31), and therefore measuring at wavelengths where the donor does not emit eliminates the luminescence of the lanthanide complex itself. The red trace in Fig. 3*B* shows an emission with a peak at ≈520 nm that corresponds to sensitized emission from fluorescein, i.e., emission resulting from LRET from Tb^{3+}, as opposed to direct fluorescein excitation. As mentioned above, the latter is essentially absent in the sample containing only fluorescein-labeled Cx43 (Fig. 3*B*, black trace). Therefore, the sensitized emission from fluorescein is easily isolated by using a bandpass emission filter (Fig. 4*A*), with negligible background fluorescence (Figs. 3*B* and 4*A*, black traces).

As expected from energy transfer, sensitized fluorescein emission increased (Fig. 4*A*) as a function of the number of acceptors per hemichannel. There was also shortening of the lifetime of the donor, which in LRET translates in the decreased sensitized emission, clearly apparent in Fig. 4*B* (see *Inset* for a direct comparison). Fig. 4*C* shows that the sensitized fluorescein emission is proportional to the number of fluorescein-labeled Cx43 per hemichannel. The LRET-based method has several advantages compared with gel filtration for the determination of the composition of purified hemichannels. First, it is more accurate because it allows for discrimination between hemichannels containing ±1 acceptor-labeled subunits (only the difference between hemichannels with two vs. three acceptor-labeled subunits was not statistically significant). This discrimination is clearly superior to that achievable with gel filtration. Second, the measurements can be carried out easily in either proteoliposomes or solution. This is very important in the case of membrane proteins because it allows for parallel determinations of oligomerization and function.

Phosphorylation by PKC of All Cx43 Hemichannel Subunits Is Needed to Abolish Sucrose Permeability. We next asked how many subunits must be phosphorylated by PKC to abolish hemichannel sucrose permeability. To accomplish this aim, we performed experiments with liposomes containing an average of 0.8 hemichannels and determined the percentage of sucrose-impermeable liposomes. If there is random exchange of connexin subunits, the distribution of the hemichannels composition will follow the binomial distribution, e.g., for a 3/3 mixture the most frequent hemichannels will contain three Cx43-dP and three Cx43-P subunits (≈31%), but there will be decreasing frequencies of 2/4 and 4/2 (≈23% each), 1/5 and 5/1 (≈9% each), and 0/6 and 6/0 (≈2% each). Proteoliposomes reconstituted with Cx43-dP hemichannels or hemichannels from Cx43-dP/Cx43-P mixtures at ratios of 5/1, 4/2, or 3/3 did not display significant sucrose retention (Fig. 5). Sucrose retention by proteoliposomes reconstituted with a 3/3 Cx43-dP/Cx43-P ratio was 6 ± 11% of the value in sucrose-impermeable proteoliposomes containing Cx43-P hemichannels (Fig. 5), although the percentage of liposomes with hemichannels containing three to six Cx43-P subunits was ≈66% according to the binomial distribution. This result indicates that the presence of three Cx43-P subunits per hemichannel yields sucrose-permeable hemichannels. Fig. 5 shows that at

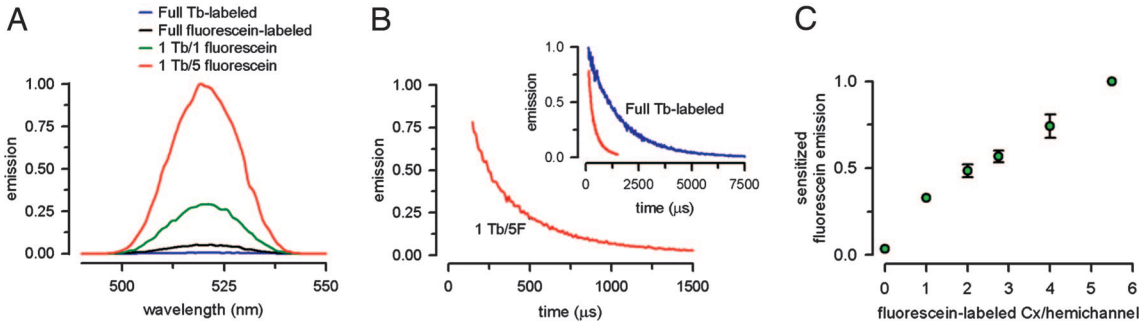

Fig. 4. Determination of hemichannel composition. (*A*) Sensitized fluorescence emission (60-μs delay after pulse), normalized as described in Fig. 3*B*. (*B*) Time course of sensitized fluorescence emission (520 ± 20 nm bandpass filter, red). (*Inset*) Donor Tb^{3+} emission (540 ± 20 nm filter, blue trace) and sensitized emission (red trace) lifetimes. Data in *A* and *B* correspond to typical traces that were obtained by using Cx43 solubilized in decylmaltoside at a concentration >1.5 mg/ml. (*C*) Sensitized fluorescence emission as a function of the average number of fluorescein-labeled connexins per hemichannel. Data were normalized to the peak value of 1 Tb/5.5 fluorescein-labeled preparation and are presented as means ± SEM of seven to nine experiments. Cx43 hemichannels were reconstituted at a ratio of 0.8 hemichannels per liposome (20 μg protein per measurement). Similar results were obtained in detergent-solubilized Cx43 at >1.5 mg/ml (data not shown), where essentially all Cx43 subunits form hemichannels (see Fig. 2). All values are statistically different from the previous one ($P < 0.001$), except for that at the 3/3 ratio. For additional details see Fig. 3.

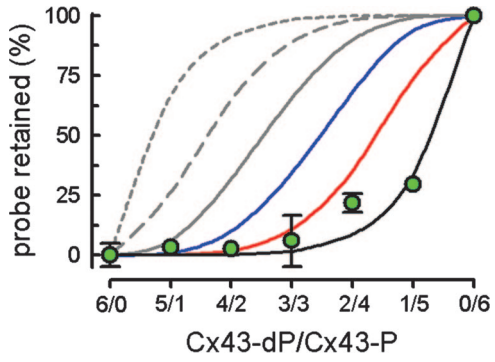

Fig. 5. Effects of the number of PKC-phosphorylated subunits per hemichannel on sucrose permeability. Effects of varying Cx34-dP/Cx43-P average ratios on the percentage of sucrose retained in proteoliposomes preloaded with the radiolabeled probe are shown. Values were normalized as described in Fig. 1. The average number of hemichannels per liposome was 0.8, and data are means ± SEM of four to seven experiments. The lines represent the percentage probe retained, expected if the number of Cx43-P subunits necessary to render the hemichannels impermeable to sucrose are ≥1 (gray, short dash), ≥2 (gray, long dash), ≥3 (gray, solid), ≥4 (blue), ≥5 (red), or 6 (black). The lines were obtained by joining with spline lines the values, calculated from the binomial distribution, for each Cx43-dP/Cx43-P mixture.

Cx43-dP/Cx43-P ratios ≤2/4 the percentage of sucrose retained was inversely proportional to the hemichannel content of Cx43-dP, but even for an average of five Cx43-P per hemichannel, sucrose retention was much less than that observed with proteoliposomes containing six Cx43-P hemichannels. For the Cx43-dP/Cx43-P reconstitution ratio of 1/5, only ≈30% of the proteoliposomes were sucrose-impermeable, although ≈83% of the Cx43 is Cx43-P in the detergent mixture. If five Cx43-Ps per hemichannel were sufficient to render the hemichannels sucrose-impermeable, then the expected sucrose-retention value would be ≈74%, the sum of the proteoliposomes containing five (≈40%) and six (≈34%) Cx43-P subunits, according to the binomial distribution. This value is significantly larger than the measured sucrose retention of 30 ± 1%, but is similar to the percentage of proteoliposomes containing six Cx43-P subunits (≈34%). These results strongly suggest that all six hemichannel subunits must be phosphorylated to abolish sucrose permeability.

It is important to consider that the equilibration time of transport probes such as sucrose across liposomes containing Cx43-dP hemichannels (1 ms) is orders of magnitude shorter than the transit of the liposomes through the gel-filtration column. Therefore, our measurements provide steady-state information on the permeability cut-off, but not on the permeation rates, needed to analyze detailed permeability changes (18). Therefore, our results cannot rule out that partial phosphorylation of the Cx43 hemichannels decreases sucrose permeability, but show that complete phosphorylation is needed to abolish sucrose permeability.

Although dynamic exchange of subunits between detergent-solubilized hemichannels was directly demonstrated by the gel-filtration and LRET experiments, the sucrose permeability studies confirmed this important observation. For example, in the absence of subunit exchange, 50% and 83% of the proteoliposomes with hemichannels reconstituted from 3/3 and 1/5 Cx43-dP/Cx43-P ratios would contain Cx43-P hemichannels impermeable to sucrose, respectively. However, the values measured were not statistically different from zero and ≈30%, respectively (Fig. 5), which is incompatible with the absence of subunit exchange, and strongly suggest that hemichannels are reconstituted in the liposomes according to their composition in detergent.

Conclusions

In this work, we described a method to generate hemichannels of controlled subunit composition by mixing detergent-solubilized connexins and show that PKC-mediated phosphorylation of all Cx43 subunits yields hemichannels that retain permeability to small hydrophilic solutes. Our results strongly suggest that for PKC to abolish permeability to larger hydrophilic solutes all six Cx43 hemichannel subunits must be phosphorylated.

The assessment of hemichannel composition using LRET and the ability to generate hemichannels of controlled subunit composition should be useful for studying disease-causing connexin mutants and assessing the effects of the isoform composition of hemichannels (heteromeric hemichannels) on permeability properties. One of the major advantages of LRET is that it can be used not only with proteins in solution, but also with lipid-reconstituted proteins. This property of LRET is essential for structural-functional studies of membrane proteins.

Materials and Methods

Cx43 Expression, Purification, Dephosphorylation, PKC-Mediated Phosphorylation, and Reconstitution. Details on the generation of recombinant baculoviruses and protein expression in High-Five insect cells have been described (18). In these studies, we used Cx43 and Cx43-EGFP (18). Protein purification was performed essentially as described (18), based on the affinity of a 6-His C-terminal tag to Ni^{2+}, but membrane solubilization and purification were carried out in decylmaltoside instead of *n*-octyl-β-D-glucopyranoside (octylglucoside). Membranes were solubilized with 1% decylmaltoside in 2 M NaCl, 10 mM EDTA, 10 mM DTT, 10 mM PMSF, and 10 mM glycine/NaOH, pH 10, at a protein concentration <2 mg/ml. During purification and subsequent steps, decylmaltoside concentration was 0.3%. To test the function of purified Cx43, we reconstituted Cx43-dP (see below) in ≈100-nm-diameter unilamellar liposomes (18) at average ratios of 0.8 or 2.3 hemichannels/liposome. Under these conditions, ≈60% and 90% of the liposomes containing Cx43-dP are predicted from the Poisson distribution to be permeable to sucrose, respectively. The experimental values, measured using a rapid filtration assay (18), were 66 ± 5 (n = 4) and 90 ± 5% (n = 7) for the 0.8 or 2.3 hemichannels/liposome average ratios, respectively. These data indicate that most, if not all, of the reconstituted hemichannels are functional, and that the fraction of purified Cx43 that can form functional hemichannels is higher than that observed when octylglucoside was the detergent (18). The analysis of the oligomeric state of Cx43 and Cx43-EGFP showed that in decylmaltoside, at protein concentrations >1 mg/ml, essentially all Cx43 and Cx43-EGFP molecules form hexamers (see Fig. 2), whereas under similar conditions in octylglucoside, 20–25% of the protein remained as monomers (18). Based on these observations and data by others (24), we decided to use decylmaltoside as the detergent of choice for Cx43 solubilization and purification. For dephosphorylation and PKC-mediated phosphorylation, we first treated purified Cx43 solubilized in decylmaltoside with immobilized alkaline phosphatase to remove phosphates from residues phosphorylated in the insect cells (18). Then, we phosphorylated a fraction of the dephosphorylated connexins with PKC, using conditions that result in phosphorylation of all of the Ser-368 residues (1 mol of Ser-368 phosphorylated per mol of Cx43) (18).

LRET Experiments. For the LRET experiments, purified WT Cx43 solubilized in 0.3% decylmaltoside was divided in three aliquots. One remained unlabeled and the others were labeled with either fluorescein maleimide (Invitrogen, Carlsbad, CA) or Tb^{3+}-DTPA-cs124-EMCH (DTPA, diethylenetriaminepentaacetate; EMCH, ε-maleimidocaproic acid hydrazide), by incubation for 2 h at 4°C with a 10-fold molar excess of the thiol reagents. Details on the

properties and synthesis (performed in the Organic Chemistry Core Laboratory at the University of Texas Medical Branch) of Tb^{3+}-DTPA-cs124-EMCH have been published (36). DTPA-cs124-EMCH contains carbostyril 124 as an "antenna" that absorbs the incident light from a nitrogen laser source and transfers it to the Tb^{3+}, which by itself displays a weak absorbance. The chelator in DTPA-cs124-EMCH, binds the lanthanide tightly and shields it from the quenching effects of water. The thiol-selective maleimide group from EMCH allows for protein labeling. After protein labeling, the unreacted compounds were removed by gel filtration, and unlabeled and labeled proteins were mixed in varying proportions and incubated for at least 2 h before the experiments. This time was sufficient for essentially complete subunit exchange between detergent-solubilized hemichannels (the subunit exchange halftime is $\approx$14 min). In some experiments, the mixtures were reconstituted into liposomes for the LRET measurements. The samples were analyzed in 100-μl quartz cuvettes. Excitation at 337 nm was carried out with a 1.45-MW pulsed nitrogen laser (GL-3300; Photon Technology International, Birmingham, NJ; 1-ns pulses at 10 Hz). Luminescence spectra were recorded on a TM11 phosphorescence lifetime system (Photon Technology International) with an R928 photomultiplier detector (Hamamatsu, Bridgewater, NJ). For most measurements, the emission monochromator was removed and replaced by band-pass filters to increase light throughput. The bandpass filters for fluorescein (XB88, 520DF10) and Tb^{3+} detection (XB91, 540DF10) were from Omega Optical (Brattleboro, VT). Steady-state fluorescence was measured on a fluorolog-2 spectrofluorometer (SPEX Industries, Edison, NJ).

Hydrophilic Solute Transport. For the transport experiments using purified Cx43 and mutants, radiolabeled probes were loaded by extrusion during the production of liposomes or proteoliposomes (18). After loading, the samples were run through a gel filtration column to remove the extraliposomal probe, and the radiolabel retained by the proteoliposomes was determined by liquid scintillation counting. The radiolabels used were ^{14}C-sucrose and ^{14}C-maltose (Amersham Biosciences, St. Louis, MO) and ^{14}C-ethyleneglycol (American Radiolabeled Chemicals, Piscataway, NJ). Background from probe trapped into compartments inaccessible for transport was assessed by permeabilization with 0.1% DMSO as described (19).

Statistics. Data are presented as means $\pm$ SEM, and statistically significant differences were assessed by Student's *t* test for paired or unpaired data, or one-way ANOVA, as appropriate.

We thank Dr. Javier Navarro for comments on the manuscript. This work was supported in part by National Institutes of Health Grants GM068586 and R21DC007150, American Heart Association Texas Affiliate Grant 0455115Y, and a grant from the John Sealy Memorial Fund for Biomedical Research.

1. Harris AL (2001) *Q Rev Biophys* 34:325–472.
2. Sosinsky GE, Nicholson BJ (2005) *Biochim Biophys Acta* 1711:99–125.
3. Unger VM, Kumar NM, Gilula NBM, Yeager M (1997) *Nat Struct Biol* 4:39–43.
4. Goldberg GS, Valiunas V, Brink PR (2004) *Biochim Biophys Acta* 1662:96–101.
5. Dhein S (2004) *Cardiovasc Res* 62:287–298.
6. Hillis GS, Duthie LA, Mlynski R, McKay NG, Mistry S, MacLeod AM, Simpson JG, Haites NE (1997) *Nephron* 75:458–463.
7. Nagy JI, Dudek FE, Rash JE (2004) *Brain Res Rev* 47:191–215.
8. John SA, Kondo R, Wang SY, Goldhaber JL, Weiss JN (1999) *J Biol Chem* 274:236–240.
9. Kondo RP, Wang SY, John SA, Weiss JN, Goldhaber JI (2000) *J Mol Cell Cardiol* 32:1859–1872.
10. Contreras JE, Sanchez HA, Eugenin EA, Speidel D, Theis M, Willecke K, Bukauskas FF, Bennett MV, Saez JC (2002) *Proc Natl Acad Sci USA* 99:495–500.
11. Vergara L, Bao X, Cooper M, Bello-Reuss E, Reuss L (2003) *J Membr Biol* 196:173–184.
12. Li WE, Nagy JI (2000) *Eur J Neurosci* 12:2644–2650.
13. Retamal MA, Cortes CJ, Reuss L, Bennett MV, Saez JC (2006) *Proc Natl Acad Sci USA* 103:4475–4480.
14. Lampe PD, Lau AF (2000) *Archiv Biochem Biophys* 384:205–215.
15. Solan JL, Lampe PD (2005) *Biochim Biophys Acta* 1711:154–163.
16. Kwak BR, van Veen TA, Analbers LJ, Jongsma HJ (1995) *Exp Cell Res* 220:456–463.
17. Bao X, Altenberg GA, Reuss L (2004) *Am J Physiol* 286:C647–C654.
18. Bao X, Reuss L, Altenberg GA (2004) *J Biol Chem* 279:20058–20066.
19. Bevans CG, Kordel M, Rhee SK, Harris AL (1998) *J Biol Chem* 273:2808–2816.
20. Weber PA, Chang HC, Spaeth KE, Nitsche JM, Nicholson BJ (2004) *Biophys J* 87:958–973.
21. Gong XQ, Nicholson BJ (2001) *Cell Commun Adhes* 8:187–192.
22. Nightingale ER, Jr (1959) *J Phys Chem* 63:1381–1387.
23. Beltramello M, Piazza V, Bukauskas FF, Pozzan T, Mammano F (2005) *Nat Cell Biol* 7:63–69.
24. Kistler J, Goldie K, Donaldson P, Engel A (1994) *J Cell Biol* 126:1047–1058.
25. Cascio M, Kumar NM, Safarik R, Gilula NB (1995) *J Biol Chem* 270:18643–18648.
26. Stauffer KA, Kumar NM, Gilula NB, Unwin N (1991) *J Cell Biol* 115:141–150.
27. Stauffer KA (1995) *J Biol Chem* 270:6768–6772.
28. Ahmad S, Diez JA, George CH, Evand WH (1999) *Biochem J* 339:247–253.
29. Marheineke K, Grunewald S, Christie W, Reilander H (1998) *FEBS Lett* 441:49–52.
30. Richardson J, Blunck R, Ge P, Selvin PR, Bezanilla F, Papazian DM, Correa AM (2006) *Proc Natl Acad Sci USA* 103:15865–15870.
31. Selvin PR (2002) *Annu Rev Biophys Biomol Struct* 31:275–302.
32. Cha A, Snyder GE, Selvin PR, Bezanilla F (1999) *Nature* 402:809–813.
33. Knauf PA, Pal P (2004) *Blood Cells Mol Dis* 32:360–365.
34. Posson DJ, Ge P, Miller C, Bezanilla F, Selvin PR (2005) *Nature* 436:848–851.
35. Vazquez-Ibar JL, Weinglass AB, Kaback HR (2002) *Proc Natl Acad Sci USA* 99:3487–3492.
36. Chen J, Selvin PR (1999) *Bioconjug Chem* 10:311–315.